Available online at www.sciencedirect.com

SCIENCE DIRECT®

Journal of Photochemistry and Photobiology A: Chemistry 179 (2006) 283–288

Journal of Photochemistry and Photobiology A:Chemistry

www.elsevier.com/locate/jphotochem

Fluorescence probing of aerosol OT based reverse micelles and microemulsions in *n*-alkanes (C_6–C_{16}) and quenching of Safranine-T in these systems

Karen M. Glenn, Rama M. Palepu [*]

Department of Chemistry, St. Francis Xavier University, P.O. Box 5000, Antigonish, NS, Canada B2G 2V8

Received 21 July 2005; received in revised form 11 August 2005; accepted 17 August 2005
Available online 23 September 2005

Abstract

The fluorescence quenching of Safranine-T (ST) (3,6-diamino-2,7-dimethyl-5 phenyl phenazinium chloride) by the inorganic ions Fe^{2+}, $[Fe(CN)_6]^{3-}$ and Cu^{2+} was studied in aerosol OT (AOT) reverse micelles and microemulsions in various non-polar solvents. The quenching process was exploited to calculate the Stern–Volmer quenching constants at different water/surfactant molar ratios (ω values). The fluorescent probes auramine-O and 8-anilino-1-napthalene sulfonic acid, ammonium salt (ANS) were employed to determine the minimum ω value for the transition of reverse micelles to microemulsions in various non-polar solvents, as well as at different concentrations of surfactant.

Keywords: Fluorescence; Quenching; Safranine-T; Surfactant; Reverse micelle; Microemulsion

1. Introduction

Reverse micelles and microemulsions have attracted considerable attention in recent years because they can provide “tailored-to-size micro reactors” [1] for chemical, biological and electron transfer reactions [2]. Also, water encased in such aggregates is thought to mimic water in biological membranes and proteins [3].

The surfactant aerosol OT (AOT, sodium bis(2-ethylhexyl) sulfosuccinate) has the ability to form reverse micelles without the aid of a co-surfactant and also solubilize large amounts of water, up to water: surfactant ratios $\omega = 40$–60 (where ω = moles of H_2O/moles AOT), depending on the surrounding non-polar medium. The solubilized water exhibits peculiar properties [4–6] owing to interactions with the polar heads of surfactant and the counter-ions. Various investigations have shown a transition region at molar ratios 6–10 between a reverse micellar state (where water is involved in surfactant and sodium ion hydration) and a microphase domain corresponding to a water-in-oil microemulsion (where part of the solubilized water is apparently free) [7–11].

Fluorescent probes are often used to provide information on the structure and dynamics of reverse micellar and microemulsion systems [12–18]. Micelles produce polar–non-polar interfaces where absorption and emission properties of dyes become enhanced or quenched. The photophysical properties of many dyes are influenced by micelles and reverse micelles [19].

The surfactant AOT used in this reverse micellar and microemulsion study has a great ability to solubilize relatively large amounts of water in a variety of hydrophobic and organic solvents. The AOT reverse micelles are also well defined with respect to size, shape and aggregation number [20–22].

Safranine-T has previously been used to study aqueous micellar solutions of surfactants [23–26], as well as reverse micellar solutions [27–30]. With regards to fluorescence quenching, there are two factors that affect the mutual encounter of the probe and quencher molecules in micellar systems. They are (i) the partitioning of the fluorescent probe and the quencher between the micellar and aqueous phase, and (ii) the dynamic distribution of these species during the quenching process [31].

The present investigation studies the fluorescence quenching of Safranine-T (ST) by the inorganic ions Fe^{2+}, $[Fe(CN)_6]^{3-}$ and Cu^{2+} in reverse micelles and microemulsions comprising the anionic surfactant AOT in various non-polar solvents. Safranine-T is a cationic fluorescent dye that is insoluble in non-polar media, but highly soluble in water. Therefore, ST is present in

---

[*] Corresponding author. Tel.: +1 902 867 3886.
E-mail address: rpalepu@stfx.ca (R.M. Palepu).

1010-6030/$ – see front matter © 2005 Elsevier B.V. All rights reserved.
doi:10.1016/j.jphotochem.2005.08.028

the aqueous core of the reverse micelle or microemulsion, or at the micellar interface near the anionic AOT headgroups [32]. Previous studies [33] found that collisional quenching occurred without electron transfer when inorganic anions were used to quench the fluorescence of ST in the aqueous micellar environment of Tween non-ionic surfactants.

The fluorescent probes auramine-O (AuO) and 8-anilino-1-naphthalenesulfonic acid (ANS) were employed to determine ω', value at which the transition from reverse micelle to microemulsion occurs, as a function of n-alkane solvent chain length. Once ω' values were established, it was possible to compare quenching efficiencies in reverse micelles and microemulsions by performing quenching experiments at ω values both above and below the ω' value for a particular solvent. The inorganic ions were chosen for their known efficiency for quenching, as well as to characterize the quenching efficiency of iron in both cationic and anionic forms.

2. Experimental

Safranine-T (E. Merck) was recrystallized from an ethanol–water mixture before use. The surfactant diisooctylsodium sulfosuccinate (AOT) was purchased from Aldrich and used without further purification. Fluorescent probes auramine-O and 8-anilino-1-naphthalenesulfonic acid were also acquired from Aldrich. Hydrocarbon solvents hexane, heptane, isooctane (2,2,4-trimethylpentane), octane, decane and dodecane were Aldrich products, and nonane, undecane and tetradecane were Alfa Aesar products with stated purity >99%. The AR grade salts $K_3[Fe(CN)_6]$, $Fe(NH_4)_2(SO_4)_2$ and $CuSO_4$ were obtained from BDH chemicals and were used as fluorescence quenchers.

The concentration of the fluorescent probes was kept constant of the order of 10^{-5} mol dm^{-3} in the reverse micelle and microemulsion media. The quencher concentrations were varied in the range 1–9 mmol dm^{-3}. Triply deionized water was used in all solution preparation. All fluorescence spectra were collected on a Spex Fluoromax-3 fluorimeter using a quartz cell. The ST probe was excited at 520 nm and studied in the range 540–610 nm. The excitation and emission bandwidths were both 1.00 nm. For auramine-O, an excitation wavelength of 440 nm was used and emission was scanned in the range 450–550 nm. The bandwidths were 3.00 and 5.00 nm for excitation and emission respectively. The excitation wavelength for ANS was 346 nm, a scan range of 400–650 nm was employed and the bandwidths were 1.05 and 2.00 nm for excitation and emission, respectively.

3. Results and discussion

3.1. Determination of ω' values for AOT reverse micellar systems in various organic solvents

The fluorescent probes ANS and AuO were used to determine the minimum ω value for the transition of reverse micelles to microemulsions (termed the ω' value). The ANS probe is essentially non-fluorescent in water, but highly fluorescent in the presence of non-polar environments or macromolecules (such as reverse micelles and microemulsions) [20,34]. The fluorescence spectra of ANS in 0.5 mol dm^{-3} AOT in heptane at different ω values are shown in Fig. 1. From the spectra, a decrease in fluorescence intensity and a concurrent red shift is evident as ω increases. A plot of intensity and wavelength as a function of ω for the same system is shown in Fig. 2A and B, respectively. The breakpoint of the two plots corresponds to the ω value at which the system changes from a reverse micelle to a microemulsion (the ω' value).

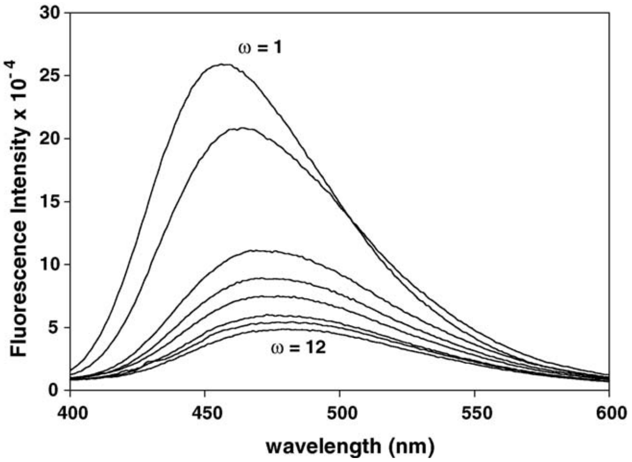

Fig. 1. Fluorescence spectra of ANS in 0.5M AOT in heptane at various ω values.

The AuO probe is sensitive to the microviscosity of its environment [35]; consequently, its fluorescence spectra display changes in intensity and position as more water is added to the reverse micellar solution. As a result, AuO fluorescence spectra can be used to determine ω' values. Results for ω' values in various non-polar solvents are reported in Table 1.

Examination of data from Table 1 indicates that ω' values decrease with increasing n-alkane solvent chain length. According to Kan-no and Kitahara [36], the solubility of water depends on the oil used because the oil can penetrate into the interface surface, increasing the critical packing parameter (v). In the absence of any specific hydrocarbon-head group interactions, the hydrocarbons that are most efficient at penetration will be those which are most similar to the surfactant tails. Therefore, the solubility of water in AOT/hydrocarbon solutions decreases as the car-

Table 1
ω' values for 0.5 M AOT in various solvents, as determined by ANS and AuO

Solvent	ω' Determined by AuO	ω' Determined by ANS
Hexane	6.3	6.2
Heptane	5.0	5.3
Octane	4.5	4.7
Nonane	4.2	4.0
Decane	3.8	3.7
Undecane	3.3	3.5
Dodecane	3.0	3.0
Tetradecane	2.8	2.4
Hexadecane	–	2.2
Isooctane	6.2	5.9
Cyclohexane	5.7	5.5

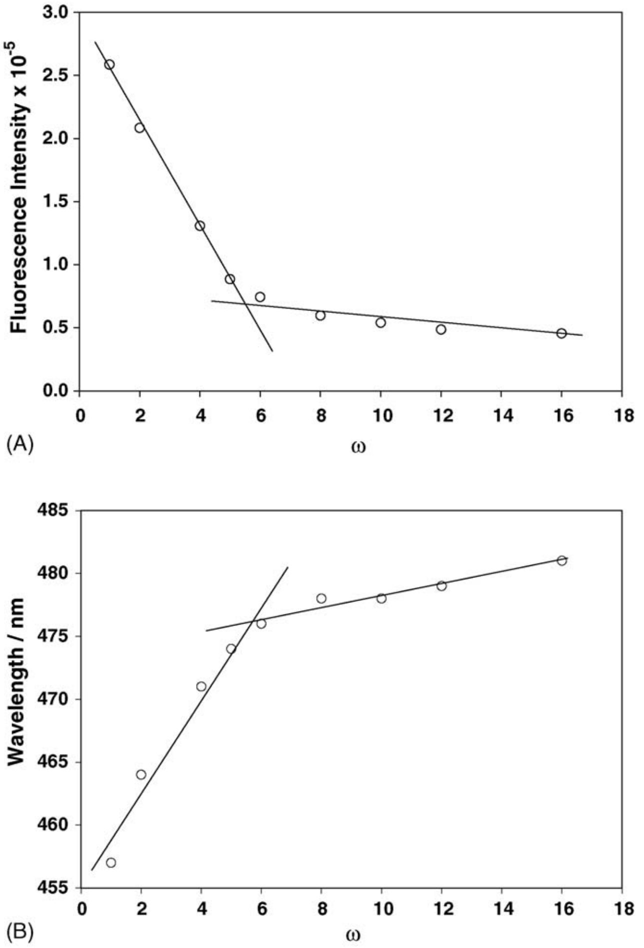

Fig. 2. 0.5 M AOT in heptane with ANS probe. (A) Fluorescence intensity vs. ω, (B) wavelength of maximum fluorescence vs. ω.

bon number of the alkane solvent increases. As a consequence, the relative droplet size is expected to decrease, along with the aggregation number, which may limit the amount of water that can be accommodated inside the core of a reverse micelle. Fig. 3 shows a plot of average ω' values versus *n*-alkane solvent chain length. The ω' values in Fig. 3 correspond to an average of the ω' values determined by following the intensity and wavelength of both ANS and AuO fluorescence spectra.

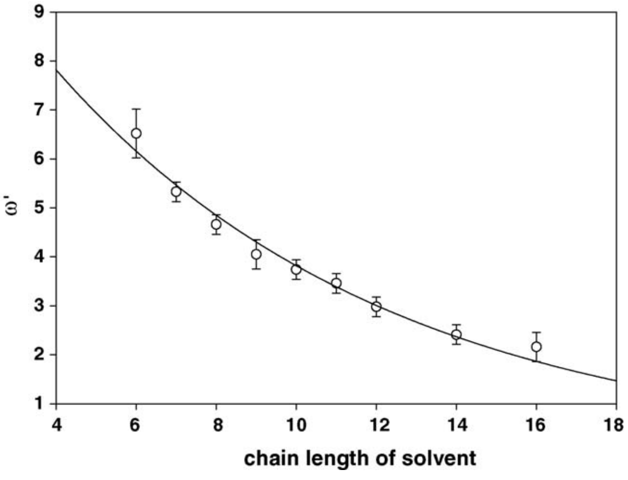

Fig. 3. Average ω'value vs. *n*-alkane solvent chain length.

Table 2
ω' values for various [AOT], as determined using ANS probe

Solvent	AOT concentration		
	0.500 M	0.375 M	0.250 M
Hexane	6.5	4.8	3.9
Heptane	5.3	4.5	3.8

The transition ω' values were also determined by ANS for various concentrations of surfactant, and the results are reported in Table 2. At lower concentrations of AOT surfactant, the aggregation numbers of the reverse micelles will be smaller [21]. Thus, less water is required to fill the hydration shells of the anionic AOT headgroups and the sodium counterions. As a result, the ω' value decreases as surfactant concentration decreases. Once the ω' values in various solvents and in different concentrations of AOT have been established, it is possible to compare the fluorescence quenching of ST by inorganic ions in reverse micelles and microemulsions.

3.2. Quenching of Safranine-T fluorescence by inorganic ions in reverse micelles and microemulsions

The Stern–Volmer quenching constants (K_{SV}) for the ions Fe^{2+}, $[Fe(CN)_6]^{3-}$, and Cu^{2+} were evaluated using the Stern–Volmer Eq. (1),

$$\frac{I_0}{I} = 1 + K_{SV}[Q] \tag{1}$$

where I_0 and I are the fluorescence intensities in absence and presence of quencher, respectively, and $[Q]$ is the concentration of quencher ion. Stern–Volmer plots of I_0/I versus $[Q]$ for the Fe^{2+} quencher are given in Fig. 4. A linear Stern–Volmer plot is indicative of a single class of fluorophore, all equally accessible to the quencher [26–28]. A decrease in K_{SV} values is observed as ω increases, with a large decrease in slope observed between $\omega = 4$ and 6 due to the formation of microemulsions. In a plot

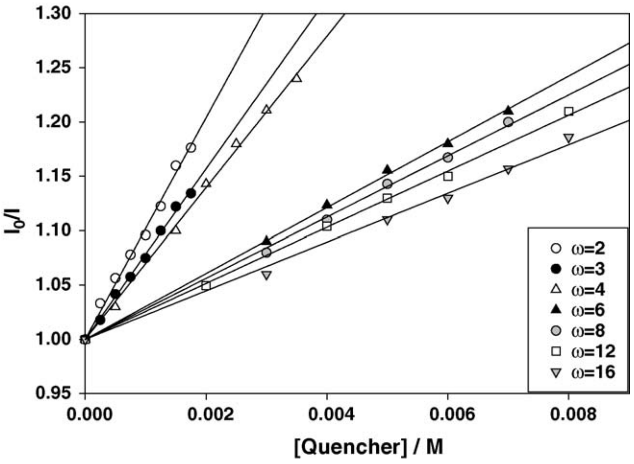

Fig. 4. Stern–Volmer plots for 0.5 M AOT in hexane, using Fe^{2+} as quencher.

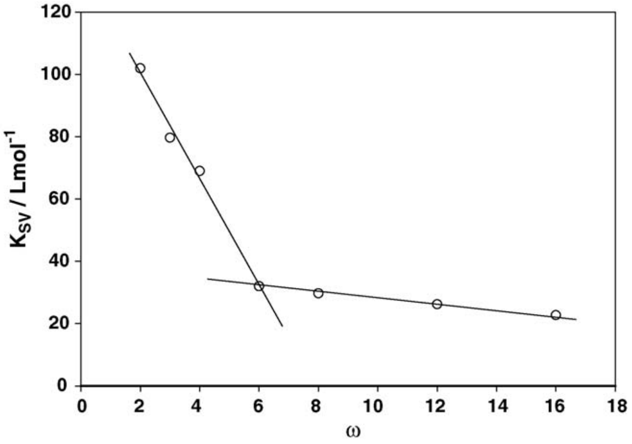

Fig. 5. K_{SV} vs. ω for 0.5M AOT in hexane, Fe^{2+} as quencher.

of K_{SV} versus ω (Fig. 5), the breakpoint corresponds to the ω' value.

In all the quenching studies performed, it was found that the K_{SV} values in reverse micelles were greater than in microemulsions. The quenching efficiency of an ion depends on its accessibility to the Safranine-T dye. In reverse micelles, the water in the core of the aggregate is bound up in sodium ion hydration, as well as in the hydration of the anionic AOT headgroups. The ST dye is not soluble in non-polar media, so it must reside in the water micropool or at the micellar interface. However, in reverse micelles, free water is absent from the micellar interior, so both the ST and the quencher ions are forced to reside at the interface. Therefore, the close proximity of the quencher and fluorophore near the interface results in efficient quenching. In microemulsions, both the quencher and the fluorophore can reside in the water pool, so the quenching efficiency is governed by the frequency of collisions between the dye and the quencher ion.

The decreasing trend of K_{SV} values with increasing ω values may also be attributed to the relative changes in the microviscosity of the waterpool. A higher microviscosity value leads to a closer proximity of the quencher ion and the dye, thereby leading to more efficient quenching. Thus, smaller K_{SV} values are observed in microemulsions than in reverse micelles.

Table 3 summarizes the K_{SV} values for the Fe^{2+} and Cu^{2+} quencher ions in 0.5 M AOT in various solvents. Generally, a decrease in K_{SV} values upon increasing the *n*-alkane solvent chain length is observed, which may be attributed to the relative degrees of hydration of the quencher ions in the various solvents.

Table 3
K_{SV} values for Fe^{2+} and Cu^{2+} in 0.5 M AOT in various *n*-alkane solvents at $\omega = 2$ and 12

Solvent	Fe^{2+} quencher		Cu^{2+} quencher	
	$\omega = 2$	$\omega = 12$	$\omega = 2$	$\omega = 12$
Hexane	102	26	54	27
Octane	95	25	48	23
Decane	98	21	40	23
Dodecane	80	18	38	20

Table 4
K_{SV} values for various quencher ions in 0.5 M AOT in isooctane

ω	Fe^{2+}	Cu^{2+}	$[Fe(CN)_6]^{3-}$
2	88	48	–
4	47	39	32
6	40	34	30
8	35	29	24
10	30	25	19
12	–	24	14
16	26	19	7

As discussed earlier, a decrease in ω' was observed as solvent chain length increases, implying that the ions may be slightly more hydrated at the same ω value in the longer chained *n*-alkane solvents.

In Table 3, it is evident that the quenching efficiencies for Fe^{2+} are greater than Cu^{2+} in reverse micelles ($\omega = 2$). The smaller size of the Fe^{2+} ion results in a higher charge density, so it may have a greater electrostatic attraction to the anionic AOT headgroups at the interface, resulting in a higher access to the dye molecule. In contrast, the K_{SV} values in microemulsions ($\omega = 12$) for the two quencher ions are similar. In microemulsions, the quencher and the fluorophore can exist in the aqueous interior; therefore the quenching efficiencies are not dependent on the size of the ions.

The K_{SV} values for various quencher ions in 0.5 mol dm^{-3} AOT in isooctane are reported in Table 4. Again, a decrease in K_{SV} values is observed as ω increases. Generally, the quenching efficiency follows the order $Fe^{2+} > Cu^{2+} > [Fe(CN)_6]^{3-}$. This trend does not follow the order of the hydrated radii [27]. Similar results were reported in the literature [27], and the reason for this trend remains unclear at this stage and requires further investigation.

All Stern–Volmer plots for the quencher ions were found to be linear, suggesting that collisional (dynamic) quenching plays the major role in the quenching process. During a collision between quencher and fluorophore, there is a possibility of electron transfer occurring. However, the metal ions Cu^{2+} and Fe^{3+} (of the ferricyanide ion) are in their maximum oxidation states and are therefore unable to undergo electron transfer. However, since these ions were still able to quench, it can be assumed that their mechanism is purely collisional and that electron transfer did not occur.

3.2.1. *Effects of surfactant concentration on the quenching of ST by Fe^{2+} and $[Fe(CN)_6]^{3-}$ in AOT reverse micelles and microemulsions*

Quenching experiments were carried out at various concentrations of AOT to further investigate the quenching processes. The K_{SV} values for Fe^{2+} and $[Fe(CN)_6]^{3-}$ in different concentrations of surfactant were obtained at constant ω values (Table 5).

It is apparent from Table 5 that a decrease in K_{SV} values for both the Fe^{2+} and $[Fe(CN)_6]^{3-}$ ions occurs upon increasing the concentration of AOT. This trend may be due to the varying viscosities of the surfactant solutions, which can be estimated using the AuO fluorescent probe. It has been established in the litera-

Table 5
K_{SV} values for Fe^{2+} and $Fe(CN)_6{}^{3-}$ quenchers at various [AOT] at $\omega = 4$ and 10

[AOT] (M)	$\omega = 4$		$\omega = 10$	
	Fe^{2+}	$Fe(CN)_6{}^{3-}$	Fe^{2+}	$Fe(CN)_6{}^{3-}$
0.125	113	–	58	84
0.250	70	99	41	42
0.375	50	46	35	35
0.500	47	32	30	19

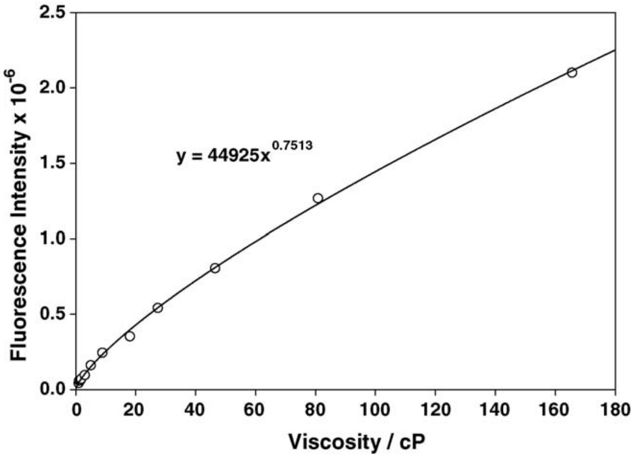

Fig. 6. Auramine-O fluorescence intensity vs. viscosity for glycerol/water system.

ture [37] that AuO can be used to estimate the microviscosity in macromolecules and membranes. AuO dissipates its electronic energy through intramolecular rotations; hence there is a correlation between fluorescence intensity and microviscosity [38]. A standard curve was constructed by measuring the fluorescence intensity of auramine-O for a series of solutions of known viscosity. Fig. 6 shows this relationship for a glycerol–water system.

The standard curve in Fig. 6 was used to estimate the viscosity of reverse micellar solutions at various concentrations of AOT, as well as at different ω values. The results are reported in Table 6. The results show that viscosity increases upon increasing the concentration of AOT. In a more viscous solution, the collisions between the fluorophore and quencher are less probable. Therefore, the decrease in K_{SV} values with increasing concentration of AOT may be attributed to viscosity effects. The standard curve in Fig. 6 can also be used to find the ω' value of reverse micellar systems, as Fig. 7 demonstrates. The breakpoint in Fig. 7 agrees well with the ω' value obtained by other methods thereby further substantiating that the non-linear standard curve fit, is a good one.

Table 6
Auramine-O fluorescence intensities and estimated viscosities

[AOT] (mol dm^{-3})	Intensity	Viscosity (cP)
0.500 ($\omega = 12$)	289262	12.0
0.500 ($\omega = 4$)	760959	43.2
0.125 ($\omega = 4$)	100499	2.9

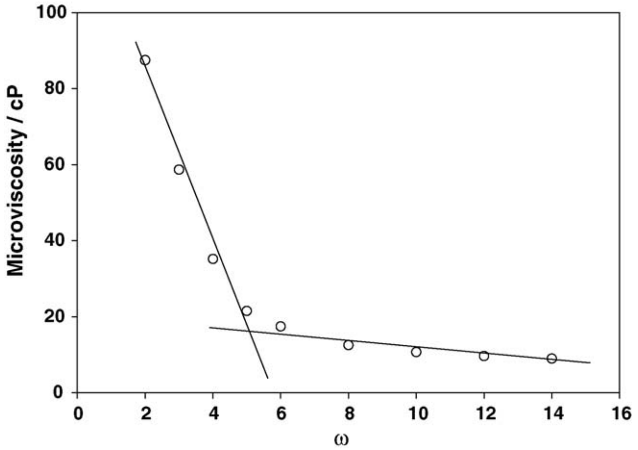

Fig. 7. ω vs. microviscosity for 0.5 M AOT in heptane using auramine-O as probe.

Another interesting trend seen in Table 5 is that the Fe^{2+} ion quenches better than $[Fe(CN)_6]^{3-}$ at lower concentrations of AOT, while the reverse trend is evident at higher concentrations. At low concentrations of AOT, there are less AOT headgroups available to shelter the ST fluorophores, implying that a greater proportion of the dye must reside in the watery core of the reverse micelle. The anionic quencher $[Fe(CN)_6]^{3-}$, being repelled by the anionic AOT headgroups, is able to quench the ST in the watery core quite efficiently and therefore can quench better at lower concentrations of surfactant. The cationic quencher Fe^{2+}, being attracted to the headgroups, has more access to the sheltered ST fluorophores and therefore it quenches better than $[Fe(CN)_6]^{3-}$ at higher concentrations of AOT.

4. Conclusions

The ω' values were determined for various non-polar solvents and for different concentrations of surfactant using ANS and AuO as fluorescent probes. It was observed that the ω' values decrease as the chain length of the *n*-alkane solvent increases, and as the concentration of AOT decreases.

The quenching of Safranine-T by inorganic ions was carried out in AOT reverse micelles and microemulsions in various non-polar solvents. The ions employed, $[Fe(CN)_6]^{3-}$, Fe^{2+} and Cu^{2+}, were all found to quench the fluorescence of ST. The Stern–Volmer constants were determined and it was found that the K_{SV} values were enhanced in reverse micelles as compared to microemulsions.

Microviscosity of the water micropool was estimated using the AuO probe, and it was found that the trend of decreasing K_{SV} values with increasing surfactant concentration may be attributed to an increased viscosity.

In 0.5 M AOT, the quenching efficiency of the ions followed the order $Fe^{2+} > Cu^{2+} > [Fe(CN)_6]^{3-}$. However, at lower concentrations of AOT, it was found that the $[Fe(CN)_6]^{3-}$ ion quenches more efficiently than the Fe^{2+} ion. This was explained in terms of electrostatic repulsions and attractions of the quencher ions with the anionic AOT headgroups.

Acknowledgements

RP acknowledges the generous support from Natural Sciences and Engineering Research Council (NSERC) in the form of Discovery grant. KG acknowledges the Undergraduate Summer Research Award (USRA) from NSERC for the year 2004. The authors are also grateful to both reviewers for their suggestions to improve the quality of this manuscript.

References

[1] P.L. Liusi, B.E. Straubs (Eds.), Reverse Micelles, Plenum Press, New York, 1984.
[2] C.J. O'Connor, T.D. Lomax, R.E. Ramage, Adv. Colloid Interface Sci. 20 (1984) 21.
[3] J.H. Fendler, Ann. Rev. Phys. Chem. 35 (1984) 173.
[4] H.F. Eicke, Chimia 36 (1982) 24.
[5] M. Wong, J.K. Thomas, T. Nowak, J. Am. Chem. Soc. 99 (1977) 4730.
[6] H.F. Eicke, J. Rehak, Helv. Chim. Acta 59 (1976) 2883.
[7] M. Zulauf, H.F. Eicke, J. Phys. Chem. 83 (1979) 48.
[8] E. Keh, B. Veleur, J. Colloid Interface Sci. 79 (1981) 465.
[9] E. Bandez, E. Monnier, B. Valeur, J. Phys. Chem. 89 (1985) 5031.
[10] J. Peyrelasse, C. Boned, J. Phys. Chem. 89 (1985) 370.
[11] M.P. Pileni, B. Hickel, C. Ferradini, J. Pucheault, Chem. Phys. Lett. 92 (1982) 308.
[12] S. Biswas, S.C. Bhattacharya, S.P. Moulik, J. Colloid Interface Sci. 271 (2004) 157.
[13] J. Czapkiewicz, M. Dlugolecka, B. Tutaj, J. Colloid Interface Sci. 276 (2004) 227.
[14] R. Kanzaki, Y. Umebayashi, T. Maki, S. Ishiguro, J. Sol. Chem. 33 (6/7) (2004) 699.
[15] T.A. Fayed, Colloids Surf. A: Physicochem. Eng. Aspects 236 (2004) 171.
[16] G. Saroja, A. Samanta, Chem. Phys. Lett. 246 (1995) 506.
[17] S. Biswas, S.C. Bhattacharya, B.B. Bhowmik, S.P. Moulik, J. Colloid Interface Sci. 244 (2001) 145.
[18] E.A. Lissi, E.B. Abuin, M.A. Rubio, A. Ceron, Langmuir 16 (2000) 178.
[19] S.M. Andrade, S.M.B. Costa, J. Photochem. Photobiol. Sci. 1 (2002) 500.
[20] M. Wong, J.K. Thomas, M. Gratzel, J. Am. Chem. Soc. 98 (9) (1976) 2391.
[21] S.P. Moulik, B.K. Paul, Adv. Colloid Interface Sci. 78 (1998) 99.
[22] T.K. De, A. Maitra, Adv. Colloid Interface Sci. 59 (1995) 95.
[23] S.C. Bhattacharya, H. Das, S.P. Moulik, J. Photochem. Photobiol. A: Chem. 74 (1993) 239.
[24] S.K. Ghosh, P.K. Khatua, J.K. Ghosh, S.C. Bhattacharya, Spectrochim. Acta Part A 61 (2005) 395.
[25] S.K. Ghosh, P.K. Khatua, S.C. Bhattacharya, Int. J. Mol. Sci. 4 (2003) 562.
[26] P. Ray, S.C. Bhattacharya, S.P. Moulik, J. Photochem. Photobiol. A: Chem. 116 (1998) 85.
[27] S. Nandi, S.C. Bhattacharya, J. Mol. Liq. 89 (2000) 223.
[28] S.C. Bhattacharya, S. Nandi, J. Surf. Sci. Technol. 12 (1996) 63.
[29] S. Nandi, S.C. Bhattacharya, Colloids Surf. A: Physicochem. Eng. Aspects 186 (2001) 179.
[30] S. Nandi, S.C. Bhattacharya, S.P. Moulik, Indian J. Chem. 39A (2000) 589.
[31] K. Kalyansudaram, Photochemistry in Microheterogenous Systems, Academic Press, New York, 1987.
[32] S.C. Bhattacharya, H. Das, S.P. Moulik, J. Photochem. Photobiol. A: Chem. 79 (1994) 109.
[33] S.A. Moore, S.E. Moore, K. Glenn, S.C. Bhattacharya, R. Palepu, Can. J. Chem. (2005) (in review).
[34] J.R. Lackowicz, Principles of Fluorescence Spectroscopy, Plenum Press, New York, 1983.
[35] S. Miyagishi, T. Asakawa, M. Nishida, J. Colloid Interface Sci. 115 (1) (1987) 199.
[36] K. Kon-no, A. Kitahara, J. Colloid Interface Sci. 37 (1971) 469.
[37] G. Oster, Y. Nishijimam, J. Am. Chem. Soc. 78 (1956) 1581.
[38] A.G. Mwalupindi, A. Rideau, R.A. Agbaria, I.M. Warner, Talanta 41 (4) (1994) 599.